Heliyon 9 (2023) e16313

Contents lists available at ScienceDirect

Heliyon

journal homepage: www.cell.com/heliyon

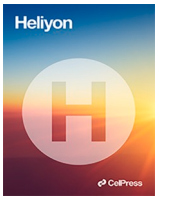

Research article

Study on the effect of different additives on the anaerobic digestion of hybrid *Pennisetum*: Comparison of nano-ZnO, nano-Fe_2O_3 and nano-Al_2O_3

Hongmei Zhao [a,b,*], Haiping Pu [b], Zhaorong Yang [b]

[a] *Key Laboratory of Medicinal Chemistry for Natural Resource, Ministry of Education, Yunnan Research & Development Center for Natural Products, School of Chemical Science and Technology, Yunnan University, Kunming, 650091, PR China*
[b] *School of Science, Yunnan Agricultural University, Kunming, 650201, China*

ARTICLE INFO

Keywords:
Anaerobic digestion
Biogas production
Hybrid *Pennisetum*

ABSTRACT

The effects of three nanomaterials (ZnO, Al_2O_3, and Fe_2O_3) on the wet and dry anaerobic digestion (AD) processes of hybrid *Pennisetum* were assessed over 33 days, and the microbial communities of dry AD systems were studied. The results demonstrated that biogas production improved by 72.2% and 33.6% when nanoporous Al_2O_3 (nano-Al_2O_3) and nano-Fe_2O_3 were added during dry AD, respectively. However, biogas production decreased by 39.4% with nano-ZnO. Kinetic analysis showed that the three nanomaterials could shorten the lag phase of the AD sludge, while the 16S rRNA gene amplicon sequencing results demonstrated that microbes such as *Longilinea* and *Methanosarcina* were enriched in the nano-Al_2O_3 reactors and methanogenic communities community such as *Methanobacterium* sp., *Methanobrevibacter* sp., and *Methanothrix* sp., which were enriched in the nano-Al_2O_3 and nano-Fe_2O_3 reactors. However, the microbial community and some methanogenic communities diversity and richness were inhibited by the addition of nano-ZnO.

1. Introduction

In recent years renewable sources of energy have drawn significant attention due to the lack of fossil fuels [1,2]. Biomass energy, such as lignocellulosic materials, livestock wastes, and sludge, has attracted increasing attention [3,4]. Hybrid *Pennisetum* (HP) is a lignocellulosic material and one of the most suitable perennial energy grasses due to its higher biogas production and good resistance, making it a promising substrate for biogas production. However, it is difficult to utilize in anaerobic digestion due to its complex structure [5–7]. Anaerobic digestion (AD) is one of the best technologies for degrading lignocellulosic materials to convert biomass energy into biogas. It includes four stages: hydrolysis, acidogenesis, acetogenesis, and methanogenesis [8]. There are two types of AD processes, namely wet anaerobic digestion and dry anaerobic digestion. In the wet anaerobic digestion system, the total solid (TS) will be less than 15%, and the value of TS in the dry AD system will be higher than 15%. However, AD has some disadvantages, such as a long reaction time, a lower production rate of methane, and a low degradation rate of organic matter [9]. Therefore, some strategies, such as additives [10,11], pretreatment [12–16], and co-digestion [17], have been used to improve biogas production and AD

* Corresponding author. Key Laboratory of Medicinal Chemistry for Natural Resource, Ministry of Education, Yunnan Research & Development Center for Natural Products, School of Chemical Science and Technology, Yunnan University, Kunming, 650091, PR China.
E-mail address: 1048354649@qq.com (H. Zhao).

https://doi.org/10.1016/j.heliyon.2023.e16313
Received 23 December 2022; Received in revised form 10 May 2023; Accepted 12 May 2023
Available online 25 May 2023

performance.

Nanomaterials as additives have been applied to the AD process because of their unique properties [18,19]. Fe_2O_3 and Al_2O_3 nanoparticles have also been used in industrial and medical products, and they were released from these products when they came into contact with water [20–22]. Ünşar et al. reported that Fe_2O_3 and Al_2O_3 nanoparticles had no impact on the AD of waste-activated sludge in short term toxicity tests, and nano-Al_2O_3 could improve biogas production. However, the reason was not clear [21]. In 2020, Chen et al. reported that AD processing could be affected by adding conductive nanomaterials, and the results showed that biogas production improved when nano-carbon powder and nano-Al_2O_3 particles were added to the AD process [22]. Nano-ZnO have been widely used in various industries, including in cosmetics, paints, plastics [23,24]. ZnO nanoparticles, the production of which could reach 550 tons per year, were found to easily remain in the waste sludge. Furthermore, the effect of waste-activated sludge on anaerobic digestion through ZnO addition has been reported. For example, the mechanism of toxicological change of ZnO and TiO_2 in AD was investigated by Zheng et al. The study showed that ZnO engineered nanoparticle materials clearly inhibited the metabolism of volatile fatty acids and biogas production in the system due to Zn^{2+} and reactive oxygen species [23]. Zhang et al. used cationic polyacrylamide to alleviate the inhibitory effects of ZnO nanoparticles on AD. The results showed that cationic polyacrylamide could reduce the toxicity of ZnO nanoparticles and the inhibition rate changed from 28.6% to 9.3% [24]. In addition, there were also another additives, such as carbon nanotubes. Carbon nanotubes could improve methane production by stimulate the biodegradation of volatile fatty acids or promot Direct Interspecies Electron Transfer (DIET) in complex anaerobic microbial communities [25,26].

Although many scholars have paid special attention to the study of AD with nanoparticles, the influence of three nanomaterials on the AD performance of HP and microbial community has not yet been investigated. In this study, the effects of three nanoporous materials (nano-ZnO, nano-Fe_2O_3, and nano-Al_2O_3) were investigated on the dry and wet AD processes, and microbial communities of the AD system. The purpose of this study was to (a), investigate the AD performance of HP, including biogas production, pH, and coenzyme F_{420} with different nanomaterials in the two AD processes, and (b), investigate and analyze the bacterial community and methanogenic communities structure of nano-ZnO, nano-Fe_2O_3 and nano-Al_2O_3 reactors during the dry AD processing.

2. Materials and methods

2.1. Raw materials (HP) and inoculum (dehydrated sludge)

The aboveground portion of HP was used for experimentation and was obtained from an experimental field at Yunnan Agricultural University. The dehydrated sludge was obtained from the fifth water purification plant in Kunming, Yunnan Province. The total solid (TS) content and the volatile solid (VS) content of the HP and sludge were tested, as shown in Table 1. The C/N ratio of HP was (31.15 ± 0.96)% (shown in Table 2), and carbon (C) and nitrogen (N) played a key role in AD and could affect microbial growth. Choosing the optimal C/N ratio was very important, and according to previous literature, the C/N ratio of 20%–30% was best [27]. Thus, the C/N ratio of HP was optimal.

2.2. Experiment

The digestion device consisted of a 1-L reaction bottle (Fig. 1), gas bottle, water bottle, and constant-temperature water bath [(37 ± 1) °C]. According to the experiment design, different amounts of nanomaterials (0.1 g, 0.2 g and 0.3 g) were added to the dry and wet AD systems. In this paper, we only chose the dry and wet AD systems with adding 0.3 g nanomaterials because the variation of biogas production is relatively obvious. Each fermentation experiment was conducted in parallel with three groups. In wet AD systems, four reactors were set, namely, the control [without nanomaterials, S-0], nano-ZnO(S-1), nano-Fe_2O_3(S-2), and nano-Al_2O_3 (S-3) materials. In dry AD systems, four reactors were set, namely, the control [without nanomaterials, G-0], nano-ZnO(G-1), nano-Fe_2O_3(G-2), and nano-Al_2O_3 (G-3) materials. All experiments were incubated at 37 °C for 33 days.

2.3. Nanomaterials synthesis

Polymethyl acrylate (PMMA) was synthesized according to the literature [28], and the nano-ZnO were synthesized by the impregnation method. First, $ZnC_2O_4{\cdot}2H_2O$ (1 g) was dissolved in methanol (10 mL), filter and then the filtrate was dropped into the PMMA (20 g) and the samples were dried 30 min at room temperature. Second, the ethanol solution of oxalic acid (3.6 g of oxalic acid dissolved in 30 mL of ethanol) were dropped into the PMMA and soak for 2min. Finally, this samples were dried in a vacuum oven at 70 °C over night. The PMMA templates were removed by calcination in flowing air keeping at 300 °C for 3 h, and then at 400 °C for 4 h, respectively. The nano-Fe_2O_3 were synthesized by the impregnation method, where $FeC_2O_4{\cdot}2H_2O$ (2 g) was dissolved in H_2O (5 mL) and $H_2C_2O_4$ (2 g) was added. Then, H_2O_2 was added dropwise until the solid was completely dissolved and ethanol (5 mL) was subsequently added to the mixture solution. Finally, this solution was dropped into the PMMA microsphere templates (20 g) and the

Table 1
The TS and VS of the HP and sludge.

Raw materials	TS (%)	VS (%)
Hybrid *Pennisetum*	94.38 ± 0.17	89.82 ± 0.45
Sludge	51.71 ± 0.21	10.09 ± 0.16

Table 2
Element content analysis of HP.

Raw materials	Element content		
	C (%)	N (%)	C/N (%)
HP	47.350 ± 0.04	1.520 ± 0.02	31.15 ± 0.96

Table 3
The design of the experiments in wet AD systems.

Reactors	Substrate	Inoculum		The amounts of additives
		Water	Sludge	
Control (S-0)	33.25 g	62.5 g	154.25 g	0
S-1	33.25 g	62.5 g	154.25 g	0.3 g
S-2	33.25 g	62.5 g	154.25 g	0.3 g
S-3	33.25 g	62.5 g	154.25 g	0.3 g

Table 4
The design of the experiments in dry AD systems.

Reactors	Substrate	Inoculum		The amounts of additives
		Water	Sludge	
Control (G-0)	30 g	20 g	200 g	0
G-1	30 g	20 g	200 g	0.3 g
G-2	30 g	20 g	200 g	0.3 g
G-3	30 g	20 g	200 g	0.3 g

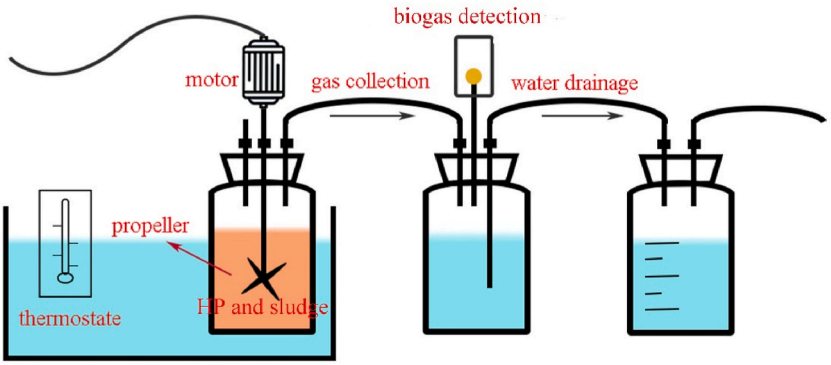

Fig. 1. The devices for anaerobic digestion.

sample was dried at 70 °C. The PMMA templates were also removed by calcination in flowing air keeping at 300 °C for 3 h, and then at 450 °C for 4 h, respectively. The nano-Al_2O_3 porous materials were also synthesized by the impregnation method, where $AlCl_3{\cdot}6H_2O$ (1.272 g) was dissolved in 10 mL ethanol, the solution was added into PMMA. The templates were fully impregnated for about 3 min, the excess solution was removed by suction. And then $NH_3{\cdot}H_2O$ (25%, 5 mL) was dropped into PMMA (20 g). The sample was finally dried at 70 °C and then calcined at 300 °C for 3 h, and then at 550 °C for 4 h, respectively.

2.4. SEM observation of the three nanomaterials

The morphology of the samples were observed by XL30 ESEM-TMP scanning electron microscope (SEM) and Zeiss Sigma scanning electron microscope.

2.5. Analytical methods

The values of pH were monitored by pH meter (OHAUS, ST3100C). TS, and VS were measured according to the standard methods [29]. The analytical method of F_{420} was previously described in the literature [30]. The total carbon (TC) and total nitrogen (TN) were measured by an elemental analysis instrument (VARIOEL III, Germany), and 16s rRNA gene amplification sequencing was obtained

using an NGS Illumina MiSeq 2 x 300 bp.

2.6. 16S rRNA gene amplicon sequencing

2.6.1. The V4 region of the bacteria

21 samples were collected on different dry AD periods. *The bacteria* stucture of 12 samples in the middle of AD process were chose to analysized (Fig. 6). The microbial DNA of All samples were extracted by using the method of CTAB-SDS. The remaining steps for DNA extraction were performed according to the DNA isolation kit protocol. Subsequently, the V4 variable region of the bacterial 16S rRNA gene was amplified using primers 515F (GTGCCAGCMGCCGCGGTAA)and 806R (GGACTACHVGGGTWTCTAAT), through polymerase chain reactions (PCRs) [16,31,32]. Then the Illumina pair-ended sequencing was performed on Illumina NovaSeq600 platform.

2.6.2. Methanogenic communities

DNA extraction of the different digestion period samples was conducted by an MIO-BIO Power Soil DNA isolation kit. The remaining steps for DNA extraction were performed according to the DNA isolation kit protocol. Subsequently, the mcrA gene was amplified using primers MLF 5′-GGTGGTGTMGGATTCACACARTAYGCWACAGC-3′ and MLR 5′-TTCATTGCRTAGTTWGGRTAGTT-3'. The PCRs were carried out in 10 μL of volume containing 1 × PCR buffer, 1 μL dNTPs, 1 μL primer (F/R), 1 unit of taq DNA polymerase, and a 5–50 ng of template DNA under the following cycling conditions: pre-denaturation at 94 °C for 2 min, 36 cycles of denaturation at 94 °C for 30 s, annealing at 60 °C for 30 s, and extension at 72 °C for 30 s, with a final extension at 72 °C for 5 min. Finally, the PCR products were tested through high-throughput sequencing using the Illumina MiSeq 2 x 300 bp platform.

3. Results and discussion

3.1. Scanning electron microscopy (SEM) of the three nanomaterials

The three nanomaterials were fabricated by using the PMMA templates. Fig. 2a showed the SEM image of nano-ZnO structure. The ordered structure have been destroyed after PMMA was removed. This because the crystallinity of nano-ZnO was enhanced [33] and the porous structure was collapsed. Fig. 2b presented the SEM image of the mesoporous Al_2O_3 structure after calcination at 550 °C. It was seen that the ordered structure replicated into Al_2O_3 matrix was not destroyed when PMMA templates were removed. An average pore diameter of 75 nm was obtained. The porous structures of and nano-Fe_2O_3 were damaged and they possibly exhibited high crystallinity (Fig. 2c).

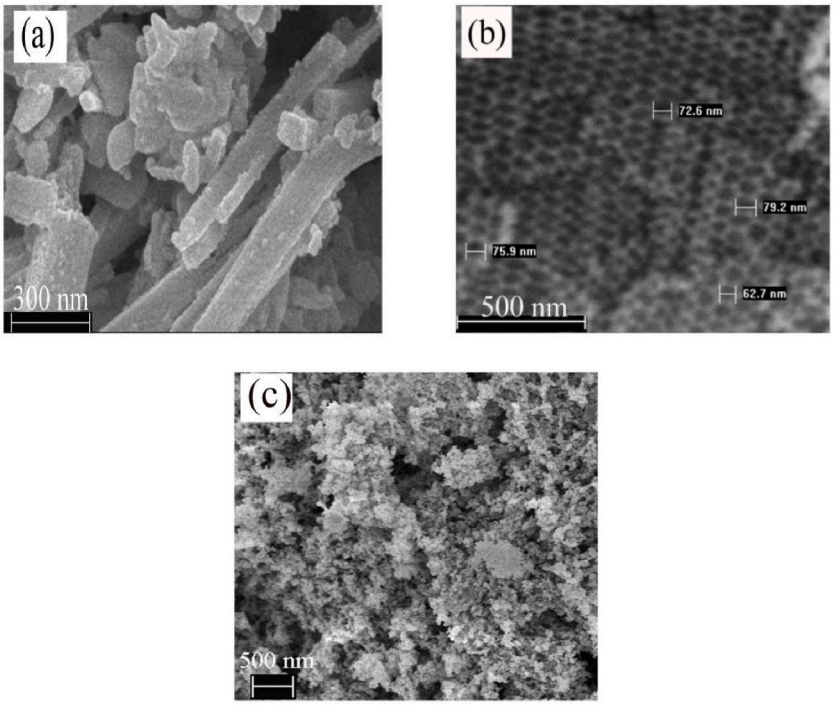

Fig. 2. SEM images of nano-ZnO (a), nano-Al_2O_3 (b) and nano-Fe_2O_3 (c).

3.2. The effect of the three nanomaterials on AD

3.2.1. Change in biogas production

In a previous study, nano-Al_2O_3 was found to be nontoxic with a positive effect on methanogenic activity, and a high concentration of nano-Fe_2O_3 could inhibit biogas production [21]. ZnO nanoparticles were found to exhibit toxicity against microorganisms and could cause a reduction in biogas production [34–36]. Fig. 3a showed the effects of three nanomaterials on daily biogas production in wet AD, where the pH values were controlled between 6.5 and 7.5 because methanogenesis could retain activity in this range. The daily biogas production values of nano-Al_2O_3 and the nano-Fe_2O_3 reactor were higher than the control (S-0) reactor. However, the value was the lowest in the nano-ZnO reactor. At about 19 days, daily biogas production in the four reactors peaked. It demonstrated the daily biogas production of the wet AD systems, which followed S-3 > S-2 > S-0 > S-1. At about 23 days, the nano-Al_2O_3 reactor peaked. As shown in Fig. 3b, the cumulative biogas production of the nano-Al_2O_3 reactor and nano-Fe_2O_3 reactor were higher than the control reactor and nano-ZnO reactor. After 33 days of experimentation, the cumulative biogas production values of the four reactors were 4404 (S-0), 3665 (S-1), 6424 (S-2), and 16,981 (S-3) mL. The cumulative biogas production of nano-Al_2O_3 was the highest. However, the biogas production of nano-ZnO decreased compared to the biogas production of control. Fig. 4 demonstrates the daily biogas production and the cumulative biogas production in the dry AD process. It can be seen that biogas yields of S-3 reactor were highest. Moreover, After 33 days of experimentation, the cumulative biogas production values of the S-3 reactor was 20,285 mL. This was higher than that of wet AD system. The biogas production of nano-ZnO decreased compared to the biogas production of control. This illustrated that porous Al_2O_3 could improve the cumulative biogas production of AD, while, the addition of nano-ZnO could inhibit biogas production [22].

The above results showed that the biogas production of wet AD and dry AD could be improved by adding nano-Fe_2O_3 and nano-Al_2O_3, especially nanoporous Al_2O_3, which could better increase the cumulative biogas production of dry AD. This was because nanoporous Al_2O_3 could serve as a good carrier for the anaerobic medium [22]. Biogas production could be inhibited when nano-ZnO was added to the wet and dry AD system. The toxicity of the ZnO nanoparticles was mainly attributed to the released Zn^{2+}, which increased the reactive oxygen species (ROS) and inhibited methane production. This explained why in this study, biogas production was inhibited by adding nano-ZnO.

3.2.2. Coenzyme F_{420} activity in the AD system

Coenzyme F_{420} is a specific enzyme that can affect the formation of methane and characterize the activity of methanogenium [37]. The results showed that the activity of coenzyme F_{420} in the nano-Al_2O_3 reactor and nano-Fe_2O_3 reactor was faster than the other two reactors. At the start of the experiment, the addition of nano-Al_2O_3 and nano-Fe_2O_3 showed no noticeable acceleration in the activity of the coenzyme F_{420}, but after 12 days, the activity of coenzyme F_{420} increased and reached a peak at 21 days (Fig. 5a and b). The activity of coenzyme F_{420} in nano-Al_2O_3 was higher, which was consistent with the experimental results of biogas production.

3.3. Kinetic study of cumulative biogas production

To analyze the kinetics of the cumulative biogas production in four reactors during dry AD, the Gompertz model were used, and the parameters are shown in Table 5. According to Table 5, it was obvious that cumulative biogas production was better fitted by this model, and R^2 was in the range of 0.96–0.99. Biogas production could be evaluated by using R_m (the maximum biogas production rate), where the R_m values of the four reactors were 207.74008 ± 4.0319 (control), 125.83007 ± 2.83418 (nano-ZnO), 312.84163 ±

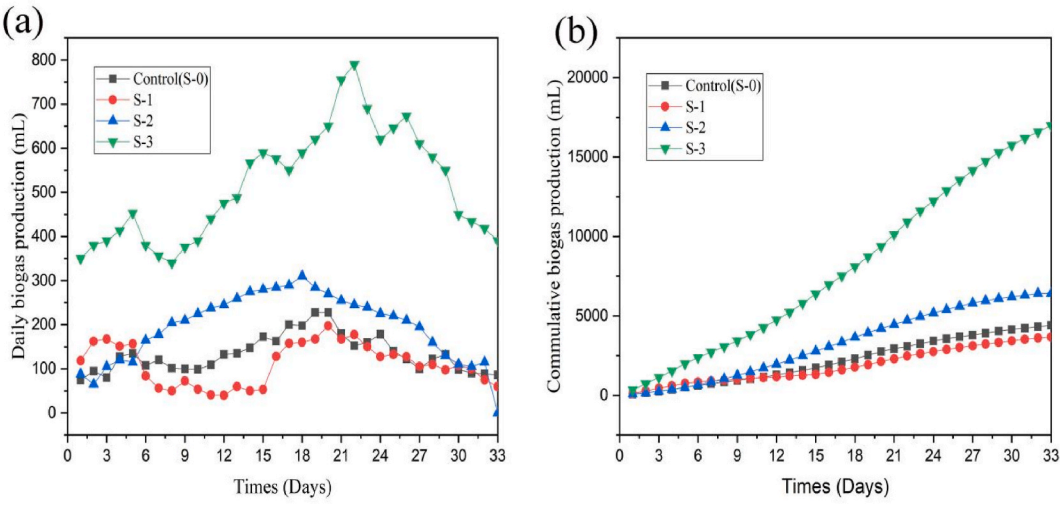

Fig. 3. The effect of daily biogas yield (a) and cumulative biogas production (b) in the wet AD system.

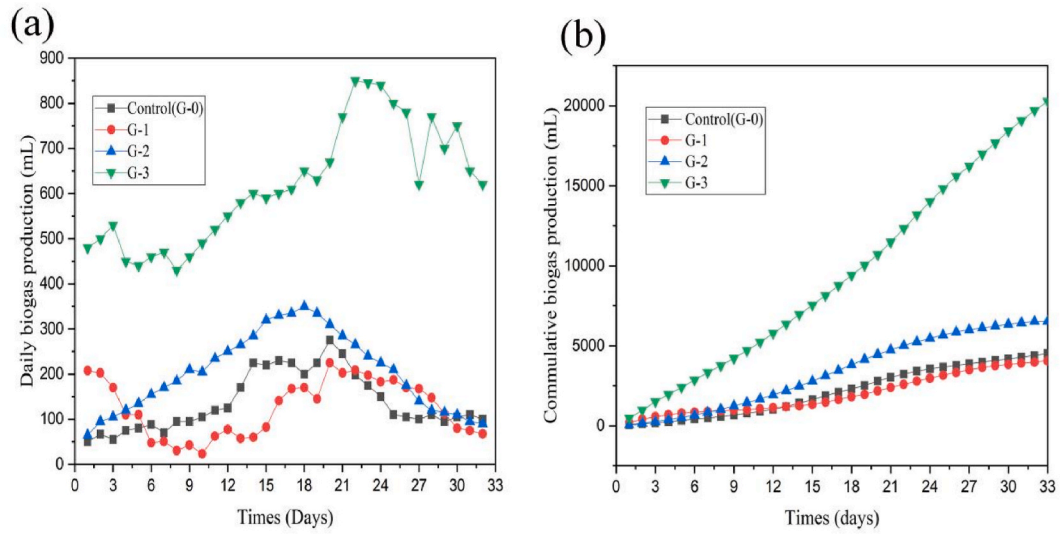

Fig. 4. The effect of daily methane yield (a) and cumulative methane production (b) in the dry AD systems.

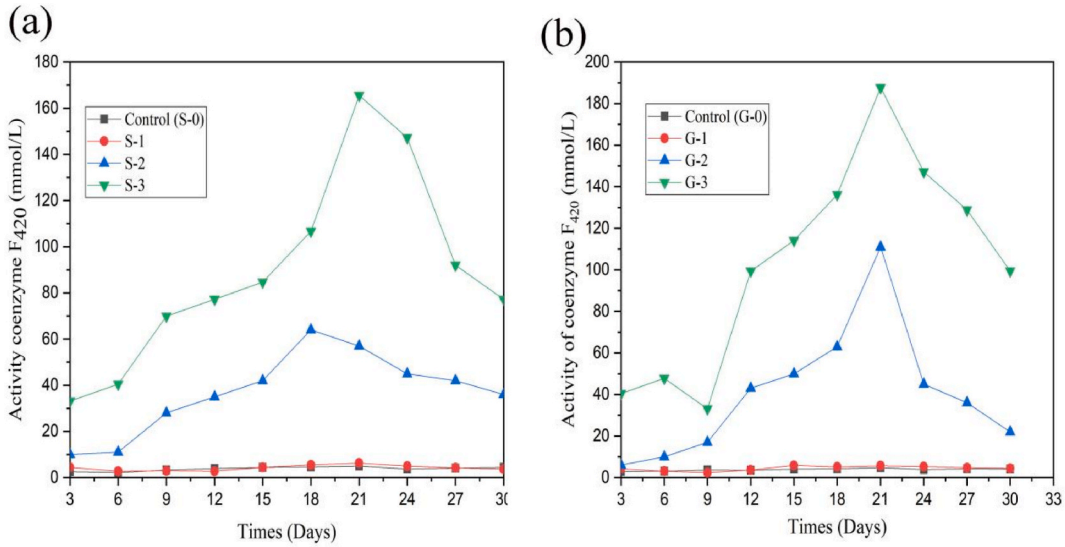

Fig. 5. Variation in coenzyme F_{420} activity in the wet AD (a) and in dry AD (b).

Table 5
Modified Gompertz model parameters of the cumulative biogas production during dry AD systems.

Reactors	P	R_m	λ	R^2
Control	5380.90362 ± 128.26508	207.74008 ± 4.0319	6.67264 ± 0.20246	0.99747
Nano-ZnO	6671.99899 ± 1223.46151	125.83007 ± 2.83418	1 ± 0	0.96483
Nano-Fe_2O_3	7642.2958 ± 111.39486	312.84163 ± 4.76187	5.60125 ± 0.15372	0.99859
Nano-Al_2O_3	36864.89923 ± 1498.36054	748.06075 ± 7.32091	5.28101 ± 0.207	0.99892

4.76187 (nano-Fe_2O_3), and 748.06075 ± 7.32091 (nano-Al_2O_3) mL/d, respectively. The R_m values in the nano-Al_2O_3 and nano-Fe_2O_3 reactors increased by 72.2% and 33.6% more than the control reactor, respectively, but the R_m values in the nano-ZnO reactor decreased by 39.4%. The value of P followed: nano-Al_2O_3 > nano-Fe_2O_3 > control > nano-ZnO, and the values of the theoretical parameters were consistent with the experimental values. This illustrated that nano-Al_2O and nano-Fe_2O_3 had a positive impact on the AD system, and the value of λ also showed that the reaction rate of dry AD improved when the three nanomaterials were added.

3.4. Microbial community

3.4.1. Variation in bacterial community structure by adding nanomaterials during the dry AD process

Fig. 6a displayed the species composition and distribution of the bacterial community at the phylum level, which mainly consisted of 11 phyla in four reactors. The predominant phyla of the bacterial community were *Firmicutes, Bacteroidetes, Chloroflexi,* and *Proteobacteria*. *Firmicutes* played an important role in the AD process. In 2018, Cheng et al. reported that *Chloroflexi* could produce hydrolytic enzymes to degrade soluble protein and soluble polysaccharides. Obviously, *Chloroflexi* decreased in the nano-ZnO reactor, and this illustrated that the hydrolysis of soluble protein and soluble polysaccharide could be inhibited by the addition of nano-ZnO. *Bacteroidetes* play an important role in hydrolyzing polysaccharides [38]. Fig. 6b demonstrated the evolution of bacterial in genus during the middle period of dry AD process in four reactors, the top 20 abundant genera were chosen for analysis. *Longilinea* that belonged to *Chloroflexi* and *Longilinea* in nano-Al_2O_3 was higher than in the other reactors, and *Longilinea* and *lostridium_sensu_stricto_12* were also higher in the nano-Al_2O_3. These two genera were mainly related to the changes in VFA concentrations and could be used to explain the higher biogas production in the nano-Al_2O_3 [22]. In previous studies, several *genera* (*Clostridium* sp., *Lysinibacillus* sp., *Acetivibrio* sp., and *Ruminofilibacter* sp. as cellulolytic bacteria) played an important role in cellulose degradation [39].

3.4.2. Community diversity of the bacterial community

Four indices of alpha diversity in the different fermentation periods are shown in Table 6. The observed number of bacterial species followed: nano-Al_2O_3-1 > nano-Fe_2O_3-1 > control > nano-ZnO-1. The species richness could be compared according to the ACE and Chao1 indices, and Shannon's index was used to compare community diversity. The highest number of bacterial observed species (1884), ACE (2289.065), and Chao1 (2271.773) all occurred in nano-Al_2O_3-1 (the middle of anaerobic fermentation). Moreover, the Shannon and Simpson indices of nano-Al_2O_3-1 were higher, and the lowest numbers of observed species (648), Chao1 (730.940), ACE (758.788), Shannon (4.492), and Simpson (0.824) indices were observed in the nano-ZnO-1 reactor. This indicated that the greatest negative effect on this AD system occurred when nano-ZnO was added to the AD system.

Beta diversity was used to illustrate the differentiation in species composition between the different reactors in the different fermentation periods. The differences in microbial community composition were evaluated by principal coordinate analysis (PCoA), as shown in Fig. 7. The contribution rates of principal components 1 and 2 were 15.51% and 14.38%, respectively. This showed that the nano-Al_2O_3 and nano-Fe_2O_3 reactors in the middle period of AD had a high similarity rate in their bacterial structure. Maybe nano-Fe_2O_3 and nano-Al_2O_3 can reduce acids accumulation and ammonia inhibition [40]. Meanwhile, they can enhance direct interspecies electron transfer (DIET) by the methanogenesis pathways using acetate and H_2/CO_2 [25,40].

3.5. Community diversity of methanogenic communities

To further study the effects of the three nanomaterials on the methanogenic communities community structure, especially the effects of nanoporous Al_2O_3, the composition and distribution of the methane function flora community at different periods at the phylum and genus level were analyzed. Fig. 8a showed that the methane community in the seven reactors mainly included three phyla, and *Euryarchaeota* was the main phylum among all phyla in each of the reactors, and its relative abundance in nano-ZnO reactor was lower than in the CK, nano-Al_2O_3, and nano-Fe_2O_3 reactors. This was because its activity was inhibited by the addition of nano-ZnO. As shown in Fig. 8b, there were 19 genera. The dominant genera of methanogenic communities community in seven reactors were *Methanobacterium* sp., *Methanobrevibacter* sp., *Methanothrix* sp. They accounted for 56%–83% of the total methanogenic communities community. The three flora increased in nano-Fe_2O_3 and nanoporous Al_2O_3, but decreased in the CK and nano-ZnO reactors. The relative abundance values of *Methanobacterium* sp. in the seven reactors were 39.64%, 42.72%, 62.87%, 83.73%, 77.44%, 56.68%, and 83.28%, respectively. The relative abundance of *Methanobacterium* sp in nano-ZnO was obviously lower than nano-Fe_2O_3 and nanoporous Al_2O_3, because nano-Fe_2O_3 and nanoporous Al_2O_3 promoted the growth of *Methanobacterium* sp. and this was in agreement with a previous study [21]. *Methanothrix* sp. decreased about 91.88% in nano-ZnO against nano-Al_2O_3, and *Methanothrix* sp. was an acetic acid type methanogens, and consisted of a very important AD process.

4. Conclusions

Biogas production of AD improved when nano-Al_2O_3 and nano-Fe_2O_3 were added, which was inhibited by the addition of nano-ZnO. Kinetic analysis showed that three nanomaterials could shorten the lag phase of the AD sludge. Methanogenic communities such as *Methanobacterium* sp., *Methanobrevibacter* sp., and *Methanothrix* sp. were enriched in the nano-Al_2O_3 and nano-Fe_2O_3 reactors in the dry AD systems. This resulted in obviously positive effects on the AD performance of HP on the microbial community diversity and richness when nano-Al_2O_3 was added to the dry AD process.

Author contribution statement

Hongmei Zhao: Conceived and designed the experiments; Performed the experiments; Analyzed and interpreted the data; Contributed reagents, materials, analysis tools or data; Wrote the paper.

Haiping Pu; Zhaorong Yang: Analyzed and interpreted the data.

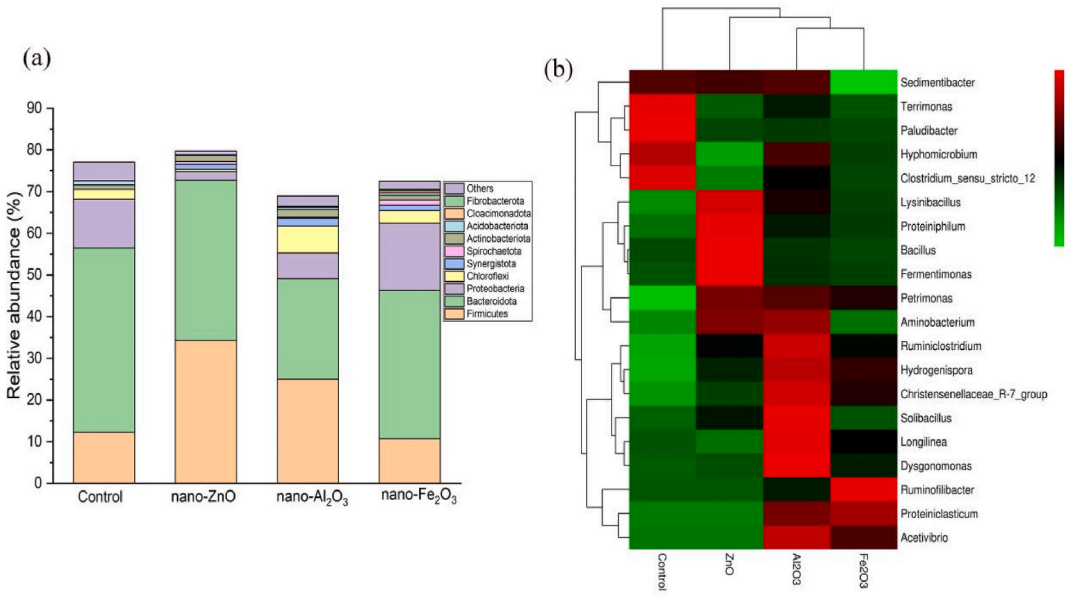

Fig. 6. The bacterial community structure at the phylum level (a) and heat map of the top 20 bacteria (b) at the genus level in the four reactors during the dry AD process.

Table 6
Indices of alpha diversity of the bacterial community at different times.

Samples	Observed species	Shannon's	Simpson's	Chao1	ACE
CK	1268	7.524	0.982	1419.068	1416.211
Nano-ZnO-1 (middle of AD)	648	4.492	0.824	730.940	758.788
Nano-ZnO-2 (late AD process)	1615	7.117	0.961	1375.306	1992.837
Nano-Fe_2O_3-1 (Middle of AD)	1832	7.95	0.985	2222.149	2221.468
Nano-Fe_2O_3-2 (late AD process)	890	5.598	0.907	993.595	1000.248
Nano-Al_2O_3-1 (middle of AD)	1884	7.878	0.980	2271.773	2289.065
Nano-Al_2O_3-2 (late AD process)	1171	6.710	0.966	1344.544	1366.874

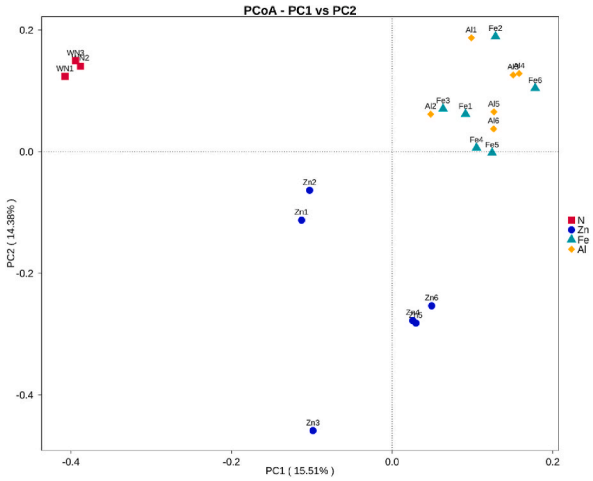

Fig. 7. Principal coordinate analysis (PCoA) of the bacteria based on the normalized OTU table, where the different colored dots represent different reactors (red: no nanomaterials; blue: AD system with added nano-ZnO; green: AD system with added nano-Fe_2O_3; orange: AD system with added nano-Al_2O_3).

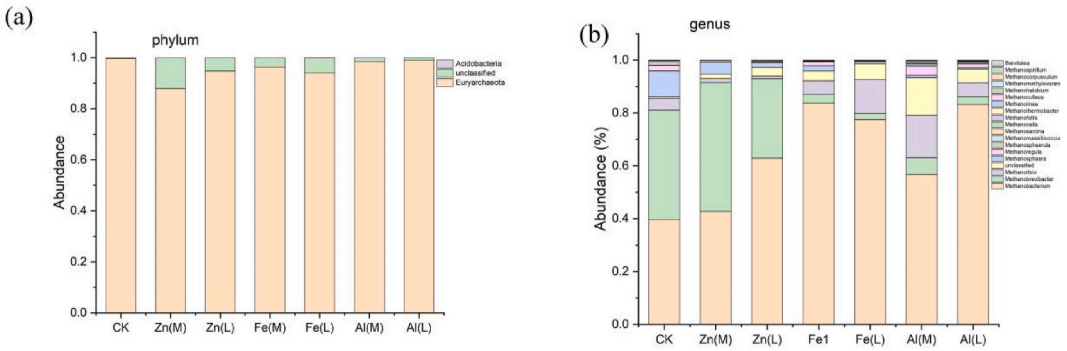

Fig. 8. Methanogenic communities community structure at the phylum level (a) and genus level (b) in different reactors with different digestion periods.

Data availability statement

The authors do not have permission to share data.

Additional information

No additional information is available for this paper.

Declaration of competing interest

The authors declare that they have no known competing financial interests or personal relationships that could have appeared to influence the work reported in this paper.

Acknowledgements

This work was supported by Agricultural Union Youth Program of Yunnan Provincial Science and Technology Department (2018FG001-102) and Scientific Research Fund of Yunnan Education Department (2023J0416). We thank Engineering and Research Center for Industrial Biogas Technology of Yunnan Province University. The archaeal diversity analysis was performed using the Omicshare tools, a free online platform for data analysis (http://www.omicshare.com/tools). We thank LetPub (www.letpub.com) for its linguistic assistance during the preparation of this manuscript.

References

[1] K.A. Nitin, K. Madan, G. Pooja, S.K. Smita, S. Lakhveer, K.V. Virendra, K. Vivek, Anaerobic digestion of sugarcane bagasse for biogas production and digestate valorization, Chemosphere 295 (2022), 133893.
[2] R.P. Venkateswara, S.S. Baral, R. Dey, S. Mutnuri, Biogas generation potential by anaerobic digestion for sustainable energy development in India, Renew. Sustain. Energy Rev. 14 (2010) 2086–2094.
[3] M. Forough, K. Keikhosro, M.J. Tohammad, Energy recovery from industrial crop wastes by dry anaerobic digestion: a review, Ind. Crop. Prod. 129 (2019) 673–687.
[4] S. Mirmohamadsadeghi, K. Karimi, I.S. Horváth, Improvement of solid-state biogas production from wood by concentrated phosphoric acid pretreatment, BioResour 11 (2016) 3230–3243.
[5] E.Y. Lim, H. Tian, Y. Chen, K. Ni, J. Zhang, Y.W. Tong, Methanogenic pathway and microbial succession during start-up and stabilization of thermophilic food waste anaerobic digestion with biochar, Bioresour. Technol. 314 (2020) 123751–123761.
[6] M. Qian, Y. Zhang, R. Li, M. Nelles, W. Stinner, Y. Li, Effects of percolate recirculation on dry anaerobic co-digestion of organic fraction of municipal solid waste and corn straw, Energy Fuel. 31 (2017) 12183–12191.
[7] K. Richa, A.K. Pandey, S. Kumar, Different aspects of dry anaerobic digestion for bio-energy: an overview, Renewable Sustainable Energy Rev. 39 (2014) 174–195.
[8] F. Momayez, K. Karimi, S. Karimi, I.S. Horváth, Efficient hydrolysis and ethanol production from rice straw by pretreatment with organic acids and effluent of biogas plant, RSC Adv. 7 (2017) 50537–50545.
[9] P.F. Li, Q. Wang, X.M. He, R. Yu, C. He, D.K. Shen, Y.Z. Jiao, Investigation on the effect of different additives on anaerobic co-digestion of corn straw and sewage sludge: comparison of biochar, Fe_3O_4, and magnetic biochar, Bioresour. Technol. 345 (2022) 126532–126542.
[10] W.Y. Li, N.A. Teck, C.N. Gek, S. Adeline, C. May, Regression analysis on ionic liquid pretreatment of sugarcane bagasse and assessment of structural changes, Biomass Bioenergy 36 (2012) 160–169.
[11] H. Thomas, S. Katrin, B. Susann, Ionic liquids as reaction medium in cellulose functionalization, Macromol. Biosci. 5 (2005) 520–525.
[12] S. Banerjee, R. Sen, R.A. Pandey, T. Chakrabarti, D. Satpute, B.S. Giri, Evaluation of wet air oxidation as a pretreatment strategy for bioethanol production from rice husk and process optimization, Biomass Bioenergy 33 (2009) 1680–1686.
[13] M. Galbe, G. Zacchi, Pretreatment of lignocellulosic materials for efficient bioethanol production, Adv. Biochem. Engin. Biotechnol 108 (2007) 41–65.
[14] Z.Z. Zhang, Y.F. Cheng, L.Z.J. Xu, Y.H. Bai, J.J. Xu, Z.J. Shi, Y.Y. Shen, R.C. Jin, Evaluating the effects of metal oxide nanoparticles (TiO_2, Al_2O_3, SiO_2 and CeO_2) on anammox process: performance, microflora and sludge properties, Bioresour. Technol. 266 (2018) 11–18.
[15] C. Cheng, Z. Zhou, Z. Qiu, J. Yang, W. Wu, H. Pang, Enhancement of sludge reduction by ultrasonic pretreatment and packing carriers in the anaerobic side stream reactor: performance, sludge characteristics and microbial community structure, Bioresour. Technol. 249 (2018) 298–306.

[16] H.S. Zheng, W.Q. Guo, Q.L. Wu, N.Q. Ren, J.S. Chang, Electro-peroxone pretreatment for enhanced simulated hospital wastewater treatment and antibiotic resistance genes reduction, Environ. Int. 115 (2018) 70–78.
[17] D.F. Wo, L.H. Li, T. Xing, Y.M. Sun, E. Jiang, Enhancement mechanisms of iron powder on co-digestion of kitchen waste and *Pennisetum* hybrid, Biochem. Eng. J. 185 (2022) 10850–10860.
[18] F. Piccinno, F. Gottschalk, S. Seeger, B. Nowack, Industrial production quantities and uses of ten engineered nanomaterials in Europe and the world, J. Nano Res. 14 (2012) 1109.
[19] S.K. Brar, M. Verma, R.D. Tyagi, R.Y. Surampalli, Engineered nanoparticles in wastewater and wastewater sludge-evidence and impacts, Waste Manag. 30 (2010) 504–520.
[20] T.M. Benn, P. Westerhoff, Nanoparticle silver released into water from commercially available sock fabrics, Environ. Sci. Technol. 42 (2008) 4133–4139.
[21] E.K. Ünşar, N.A. Perendeci, What kind of effects do Fe_2O_3 and Al_2O_3 nanoparticles have on anaerobic digestion, inhibition or enhancement? Chemosphere 211 (2018) 726–735.
[22] Y.W. Chen, Z.H. Yang, Y.R. Zhang, Y.P. Xiang, R. Xu, M.Y. Jia, J. Cao, W.P. Xiong, Effects of different conductive nanomaterials on anaerobic digestion process and microbial community of sludge, Bioresour. Technol. 304 (2020) 123016–123026.
[23] L. Zheng, Z.X. Zhang, L.P. Tian, L.L. Zhang, S.K. Cheng, Z.F. Li, Mechanistic investigation of toxicological change in ZnO and TiO_2 multinanomaterial systems during anaerobic digestion and the microorganism response, Biochem. Eng. J. 147 (2019) 62–71.
[24] B.W. Zhang, X. Tang, C.Z. Fan, W.L. Hao, Y.L. Zhao, Y.J. Zeng, Cationic polyacrylamide alleviated the inhibitory impact of ZnO nanoparticles on anaerobic digestion of waste activated sludge through reducing reactive oxygen species induced, Water Res. 205 (2021) 117651–117659.
[25] A.F. Salvador, G. Martins, M. Melle-Franco, R. Serpa, A.J.M. Stams, A.J. Cavaleiro, M.A. Pereira, M.M. Alves, Carbon nanotubes accelerate methane production in pure cultures of methanogens and in a syntrophic coculture, Environ. Microbiol. 19 (2017) 2727–2739.
[26] E.E. Ziganshina, S.S. Bulynina, A.M. Ziganshin, Anaerobic digestion of chicken manure assisted by carbon nanotubes: promotion of volatile fatty acids consumption and methane production, Fermentation 8 (2022) 641–651.
[27] L. Lin, F.Q. Xu, X.M. Ge, Y.B. Li, Chapter four - biological treatment of organic materials for energy and nutrients production—anaerobic digestion and composting, Adv. Bioenergy 4 (2019) 121–181.
[28] D. Zou, S. Ma, R. Guan, Model filled polymers. V. Synthesis of crosslinked monodisperse poly (methylmethacrylate) bead, Polym. Sci. Part A: Polym. Chem. 30 (1992) 137–144.
[29] A.D. Eaton, A.E. Greenberg, L.S. Cleseri, M.A.H. Franson, Standard Methods for the Examination of Water & Wastewater, 1995.
[30] Y.H. Cheng, S.X. Sang, H.Z. Huang, X.J. Liu, J.B. Quang, Variation of coenzyme F_{420} activity and methane yield in landfill simulation of organic waste, J. China Inst. Min. Technol. 3 (2007) 403–408.
[31] J.G. Caporaso, C.L. Lauber, W.A. Walters, D. Berg-Lyons, C.A. Lozupone, P.J. Turnbaugh, N. Fierer, Rk, Global patterns of 16S rRNA diversity at a depth of millions of sequences per sample, Proc. Natl. Acad. Sci. USA 108 (Supplement 1) (2011) 4516–4522.
[32] J. Kuczynski, J. Stombaugh, W.A. Walters, A. González, J.G. Caporaso, R. Knight, Using QIIME to analyze 16S rRNA gene sequences from microbial communities, Curr. Protoc. Bioinformat. (2011) 10.7.1–10.7.20 (Chapter 10).
[33] H.G. Zhao, C.H. Li, H.Q. Wang, R. Li, G.H. Zhang, Effects of calcination teperature on crystallization and optical properties of ZnO powder, Chin. J. Appl. Chem. 31 (2014) 188–192.
[34] N.M. Franklin, N.J. Rogers, S.C. Apte, G.E. Batley, G.E. Gadd, P.S. Casey, Comparative toxicity of nanoparticulate ZnO, bulk ZnO, and $ZnCl_2$ to a freshwater microalga (pseudokirchneriella subcapitata): the importance of particle solubility, Environ. Sci. Technol. 41 (2007) 8484–8490.
[35] S.W.Y. Wong, P.T.Y. Leung, A.B. Djurisic, K.M.Y. Leung, Toxicities of nano zinc oxide to five marine organisms: influences of aggregate size and ion solubility, Anal. Bioanal. Chem. 396 (2010) 609–618.
[36] T. Xia, M. Kovochich, M. Liong, L. Madler, B. Gilbert, H. Shi, J.I. Yeh, J.I. Zink, A.E. Nel, Comparison of the mechanism of toxicity of zinc oxide and cerium oxide nanoparticles based on dissolution and oxidative stress properties, ACS Nano 2 (2008) 2121–2134.
[37] P.J. Reynolds, E. Colleran, Evaluation and improvement of methods for coenzyme F_{420} analysis in anaerobic sludges, J. Microbiol. Methods 7 (1987) 115–130.
[38] S.M. Lauren, L.L.R. Sabina, W.G. Bjorge, E. Vincent, P.B. Pope, J. Larsbrink, Polysaccharide degradation by the Bacteroidetes: mechanisms and nomenclature, Environ. Microbiol. Rep. 13 (2021) 559–581.
[39] P.C. Burrell, C. Osullivan, H. Song, W.P. Clarke, L.L. Blackall, Identification, detection, and spatial resolution of Clostridium populations responsible for cellulose degradation in a methanogenic landfill leachate bioreactor, Appl. Environ. Microbiol. 70 (2004) 2414–2419.
[40] T. Wang, D. Zhang, L.L. Dai, B. Dong, X.H. Dai, Magnetite triggering enhanced DIET: a scavenger for the blockage of electron transfer in anaerobic digestion of high-solids sewage sludge, Environ. Sci. Technol. 52 (2018) 7160–7169.